Partial Crystallization of Mid-Ocean Ridge Basalts in the Crust and Mantle

CLAUDE HERZBERG*

DEPARTMENT OF GEOLOGICAL SCIENCES, RUTGERS UNIVERSITY, NEW BRUNSWICK, NJ 08903, USA

Pressures at which partial crystallization occurs for mid-ocean ridge basalts (MORB) have been examined by a new petrological method that is based on a parameterization of experimental data in the form of projections. Application to a global MORB glass database shows that partial crystallization of olivine + plagioclase + augite ranges from 1 atm to 1·0 GPa, in good agreement with previous determinations, and that there are regional variations that generally correlate with spreading rate. MORB from fast-spreading centers display partial crystallization in the crust at ridge segment centers and in both mantle and crust at ridge terminations. Fracture zones are likely to be regions where magma chambers are absent and where there is enhanced conductive cooling of the lithosphere at depth. MORB from slow-spreading centers display prominent partial crystallization in the mantle, consistent with models of enhanced conductive cooling of the lithosphere and the greater abundance of fracture zones through which they pass. In general, magmas that move through cold mantle experience some partial crystallization, whereas magmas that pass through hot mantle may be comparatively unaffected. Estimated pressures of partial crystallization indicate that the top of the partial melting region is deeper than about 20–35 km below slow-spreading centers and some ridge segment terminations at fast-spreading centers.

KEY WORDS: *MORB; olivine gabbro; partial crystallization; partial melting; ridge segmentation; fracture zones; crust; mantle; lithosphere*

INTRODUCTION

Early studies reached the following general conclusions concerning the origin of mid-ocean ridge basalt (MORB). Partial melting occurs in the mantle during decompression, and terminates at or near the base of the oceanic crust (e.g. Klein & Langmuir, 1987). Partial crystallization begins by the precipitation of dunite, troctolite and gabbro in the lower crust, and it ends with the solidification of the erupted lavas. However, there are a number of observations that complicate this simple picture. The occurrence of gabbro is not confined to the crust, but it is also observed as veins and segregations within residual mantle peridotite (Dick, 1989; Nicolas, 1989; Ceuleneer & Rabinowicz, 1992; Hekinian et al., 1993; Dick & Natland, 1996). Petrological evidence suggests that partial crystallization can occur in both crust and mantle (Tormey et al., 1987; Grove et al., 1992; Elthon et al., 1995; Dmitriev, 1998; Michael & Cornell, 1998). These observations imply that the top of the melting regime may not always coincide with the base of the crust (Shen & Forsyth, 1995; White et al., 2001).

One way to constrain the depth locations of the melting regime is by using the tools of petrology to model the melting process. However, this is a complex procedure that results in both low and high pressures of final melting (Klein & Langmuir, 1987; Niu & Batiza, 1991; Langmuir et al., 1992; Shen & Forsyth, 1995; Asimow et al., 2001). Assumptions must be made concerning the source composition, the melting mechanism, the modeling of partial melts from equilibrium experimental data, and how these are integrated to yield a primary aggregate MORB magma. Large uncertainties in the estimation of equilibration pressure for partial melts are propagated from relatively small uncertainties in experimental determinations of the FeO and MgO contents of liquids (Herzberg & O'Hara, 2002). Restoring candidate primary partial melt compositions from lavas that have experienced partial crystallization in the production of gabbro and troctolite is not straightforward (O'Hara & Herzberg, 2002), a problem that is revisited in the discussion below.

An alternate way of constraining the pressure at the top of the melting column is by defining where partial melting has been replaced by partial crystallization as the

*E-mail: Herzberg@rci.rutgers.edu

dominant process. Grove and coworkers (Tormey *et al.*, 1987; Grove *et al.*, 1992) were the first to explore this by directly comparing MORB compositions with experimental liquid compositions that were synthesized over a wide range of pressures. This method has the advantage of being relatively simple, and it requires fewer assumptions than models of partial melting. In this way, it was shown that some MORB might have experienced partial crystallization of Ol + Plag + Aug at depths within the mantle (Tormey *et al.*, 1987; Grove *et al.*, 1992). Dmitriev (1998) and Michael & Cornell (1998) reached similar conclusions after extending this approach to a wider MORB database. An important implication is that pressures of final melting within the melting regime are in some cases likely to be high.

The method reported below makes use of the experimental observation that the effect of pressure on the equilibrium liquid + olivine + plagioclase + augite is to dissolve relatively more plagioclase and olivine in the liquid at the expense of augite. The experimental database is parameterized in the form of projections, and pressures of partial crystallization are obtained for a global MORB database. The conclusion of Grove and coworkers that MORB can experience partial crystallization in both crust and mantle (Tormey *et al.*, 1987; Grove *et al.*, 1992) is substantiated in this work. Additionally, there are regional variations in the pressure of partial crystallization that correlate with spreading rate, a conclusion reached previously by Michael & Cornell (1998). Finally, the association made by Dmitriev (1998) of high pressures of partial crystallization with fracture zones is also corroborated. A general model is presented in which these observations are interpreted in terms of the intrinsic temperature of the crust and mantle below oceanic ridges.

OLIVINE GABBRO, TROCTOLITE AND WEHRLITE IN MORB PETROGENESIS

Olivine gabbro [olivine + plagioclase + augite] is a commonly observed lithology in samples of the lower crust in the ocean basins and ophiolite complexes (Nicolas *et al.*, 1988; Hekinian *et al.*, 1993; Dick *et al.*, 2000; Koga *et al.*, 2001). Olivine gabbro is also found in veins and segregations that crosscut upper-mantle harzburgite tectonites in the ocean basins and in ophiolites (Ceuleneer & Rabinowicz, 1992; Dick & Natland, 1996). Samples of MORB whole rocks and glasses from oceanic ridges have geochemical variations that can be related by mass balance with the removal of various amounts of olivine + plagioclase + augite (Dungan & Rhodes, 1978; Rhodes *et al.*, 1979; Fisk *et al.*, 1980; Thompson *et al.*, 1980). These same samples typically contain

phenocrysts of olivine + plagioclase (O'Hara, 1968*a*; Bryan, 1979; Thompson *et al.*, 1980), and crystallization of this assemblage can form lesser amounts of troctolite that are also observed in the ocean basins and ophiolites. The lack of augite as a phenocryst phase in MORB glass populations that require its participation by geochemical mass balance has been repeatedly noted (Dungan & Rhodes, 1978; Fisk *et al.*, 1980; Francis, 1980; Elthon *et al.*, 1995). Many workers have suggested that this 'pyroxene paradox' can be resolved by partial crystallization of augite at high pressures followed by olivine + plagioclase precipitation on eruption at the surface (O'Donnell & Presnall, 1980; Thompson *et al.*, 1980; Fujii & Bougault, 1983; Grove *et al.*, 1992; Elthon *et al.*, 1995).

The pyroxene paradox is not really very paradoxical. Experimental phase equilibrium observations show that decompression causes an expansion of the olivine and plagioclase liquidus crystallization fields at the expense of clinopyroxene (O'Hara, 1968*b*; Bender *et al.*, 1978; Presnall *et al.*, 1978, 1979; Fujii & Bougault, 1983; Grove *et al.*, 1992). Indeed, an aliquot of basalt that crystallizes olivine + plagioclase + augite in a crustal magma chamber must precipitate olivine + plagioclase at the surface even though the pressure drop may be less than 0·1 GPa. This led O'Hara (1968*a*) to conclude that MORB crystallizes olivine + plagioclase + augite near 1 atm even though olivine + plagioclase is the common phenocryst assemblage.

Wehrlite [olivine + augite] has been found as nodules in lavas from Theistareykir volcano on Iceland, and various lines of evidence have been used to indicate that they crystallized from relatively dry magmas at elevated pressures (Maclennan *et al.*, 2001, 2003). Within the Oman ophiolite wehrlite is relatively abundant, but it is restricted to intrusions at the Moho and within the overlying crust where augite appears as a cumulus phase (Nicolas *et al.*, 1988; Koga *et al.*, 2001); it does not occur in the mantle peridotites (Pallister & Hopson, 1981). Wehrlite has also been reported as impregnations in mantle harzburgite from the Hess Deep of the East Pacific Rise (Hekinian *et al*, 1993); however, Dick & Natland (1996) suggested that these differ from wehrlites in the Oman ophiolite in being volumetrically minor, and augite in the Hess Deep wehrlites does not have a cumulus origin. High magmatic water contents associated with subduction can expand the stability field of augite at the expense of plagioclase, and lead to the production of wehrlites (Gaetani *et al.*, 1993). Indeed, some basalts in the Oman ophiolite differ from MORB in displaying Nb and Ta depletions that are similar to island arc tholeiites (Lippard *et al.*, 1986). Furthermore, peridotites in the mantle section of the Oman ophiolite are enriched in SiO_2 compared with abyssal peridotites, and similar to those from subduction zones (Herzberg, 2004). The observations outlined above indicate that fractionation

of Ol + Aug and formation of wehrlite cumulates in MORB petrogenesis are likely to be unimportant.

EXPERIMENTAL DATA ON THE [LIQUID+OLIVINE+PLAGIOCLASE+ AUGITE] COTECTIC VIEWED IN PROJECTION FROM OLIVINE

It is useful to begin this analysis with analogs of the equilibrium [L + Ol + Plag + Aug] in the system CaO–MgO–Al$_2$O$_3$–SiO$_2$. This is the most simple system capable of displaying these four phases; it provides the basis for understanding basalt petrogenesis (O'Hara, 1968*b*), and it has now been extensively studied by experiment [see Longhi (1987) and Libourel *et al.* (1989) for reviews]. At 1 atm, the cotectic [L + Fo + An + Aug] contains a thermal maximum that separates liquids with low and high SiO$_2$ contents (Osborn & Tait, 1952; O'Hara & Schairer, 1963; Presnall *et al.*, 1978; Biggar, 1984; Longhi, 1987; Libourel *et al.*, 1989). Crystallization of liquids on the SiO$_2$-rich side of the thermal maximum develops elevated SiO$_2$ contents, and eventually Opx will be stabilized [L + Fo + Opx + Cpx + An] at a peritectic invariant point (Presnall *et al.*, 1979; Longhi, 1987; Libourel *et al.*, 1989; Walter & Presnall, 1994). This peritectic joins the cotectics [L + Fo + An + Aug] and [L + An + Aug + Opx] and further crystallization can yield liquids with progressively elevated SiO$_2$ (Longhi, 1987).

The effects of compositional variations and pressure on the olivine gabbro cotectic [L + Ol + Plag + Aug] are complex and have been the subject of a number of reviews (Grove *et al.*, 1992; Danyushevsky *et al.*, 1996; Yang *et al.*, 1996; Herzberg & O'Hara, 1998). In natural complex systems, the high-SiO$_2$ termination transforms from a peritectic to a distributary, and Opx is replaced by pigeonite (Grove *et al.*, 1982). Elevation of the pressure between atmospheric and 1 GPa causes both the olivine and plagioclase liquidus fields to contract (e.g. O'Hara, 1968*b*; Presnall *et al.*, 1978, 1979; Grove *et al.*, 1992). This results in liquids that are in equilibrium with olivine + plagioclase + augite to have higher MgO and Al$_2$O$_3$ as pressure increases, similar to primitive high-alumina basalts. Addition of alkalis can greatly expand the olivine liquidus field (Schairer, 1954; Schairer & Yoder, 1967; Roeder, 1974; Irvine, 1976; Biggar & Humphries, 1981; Langmuir *et al.*, 1992; Yang *et al.*, 1996), and mask any high-pressure signal, a serious problem for liquids generated at low mass fractions of melting. A simple way to recover pressure information that is typically lost from liquids with variable alkali concentrations is to view the [L + Ol + Plag + Aug] cotectic in a projection that does not include olivine as a co-ordinate. This is shown in Fig. 1 as a projection of liquids for the equilibrium

[L + Ol + Plag + Aug] to and from olivine into the plane Anorthite–Diopside–Enstatite.

The projection of liquids shown in Fig. 1 follows from the projection code described by Herzberg & O'Hara (1998). All weight percent compositions are converted to mole percent. Any Fe$_2$O$_3$ is combined with olivine (Herzberg & O'Hara, 2002). The point of projection is Olivine + Fe$_2$O$_3$ + Na$_2$O.Si$_3$O$_6$ + K$_2$O.Si$_3$O$_6$, and projection co-ordinates are calculated in the following way:

$$An = Al_2O_3 + Cr_2O_3 + TiO_2 \qquad (1)$$

$$Di = CaO + Na_2O + 3K_2O - Al_2O_3 - Cr_2O_3 \quad (2)$$

$$\begin{aligned} En = SiO_2 &- 0{\cdot}5Al_2O_3 - 0{\cdot}5Cr_2O_3 \\ &- 0{\cdot}5FeO - 0{\cdot}5MnO - 0{\cdot}5MgO \\ &- 1{\cdot}5CaO - 3Na_2O - 3K_2O - 0{\cdot}5NiO. \end{aligned} \quad (3)$$

The rationale for this projection code has been discussed previously (Herzberg & O'Hara, 1998, 2002). Liquids projected into Fig. 1 serve to calibrate the effect of pressure on the olivine gabbro cotectic [L + Ol + Plag + Aug]. Data at 1 atm are from Walker *et al.* (1979), Grove *et al.* (1982), Grove & Bryan (1983), Kinzler & Grove (1985), Mahood & Baker (1986), Baker & Eggler (1987), Tormey *et al.* (1987), Juster *et al.* (1989), Ussler & Glazner (1989), Thy & Lofgren (1992, 1994), and Yang *et al.* (1996). Data at 0·2, 0·8, and 1·0 GPa are MORB and arc tholeiite compositions from Bender *et al.* (1978), Baker & Eggler (1987), Falloon & Green (1987), Bartels *et al.* (1991), and Grove *et al.* (1992). The data of Kennedy *et al.* (1990) and Kinzler & Grove (1992) are difficult to parameterize, and have not been used in this parameterization or that of Yang *et al.* (1996).

The effect of pressure is to increase the Al$_2$O$_3$ content of liquids on the olivine gabbro cotectic, and this is manifest in higher plagioclase contents when viewed in projection. Also shown are experimental data for liquids in equilibrium with a plagioclase lherzolite analog in the system CaO–MgO–Al$_2$O$_3$–SiO$_2$ (CMAS; Walter & Presnall, 1994), which define the low-CaO pyroxene termination of the olivine gabbro cotectic [L + Fo + An + Cpx + Opx]. There is generally good internal pressure consistency between the two sets of data, demonstrating the utility of CMAS as an analog of basalts with widely variable alkali contents.

The loci of liquid compositions on the [L + Ol + Plag + Aug] cotectics shown in Fig. 1 have been parameterized from the experimental data with the following equations:

$$An = 52{\cdot}95 + 10{\cdot}08P + 1{\cdot}58P^2 - 0{\cdot}4645En \quad (4)$$

$$An + En + Di = 100 \qquad (5)$$

where An and En are molecular projection co-ordinates defined in equations (1) and (3), and *P* is in units of
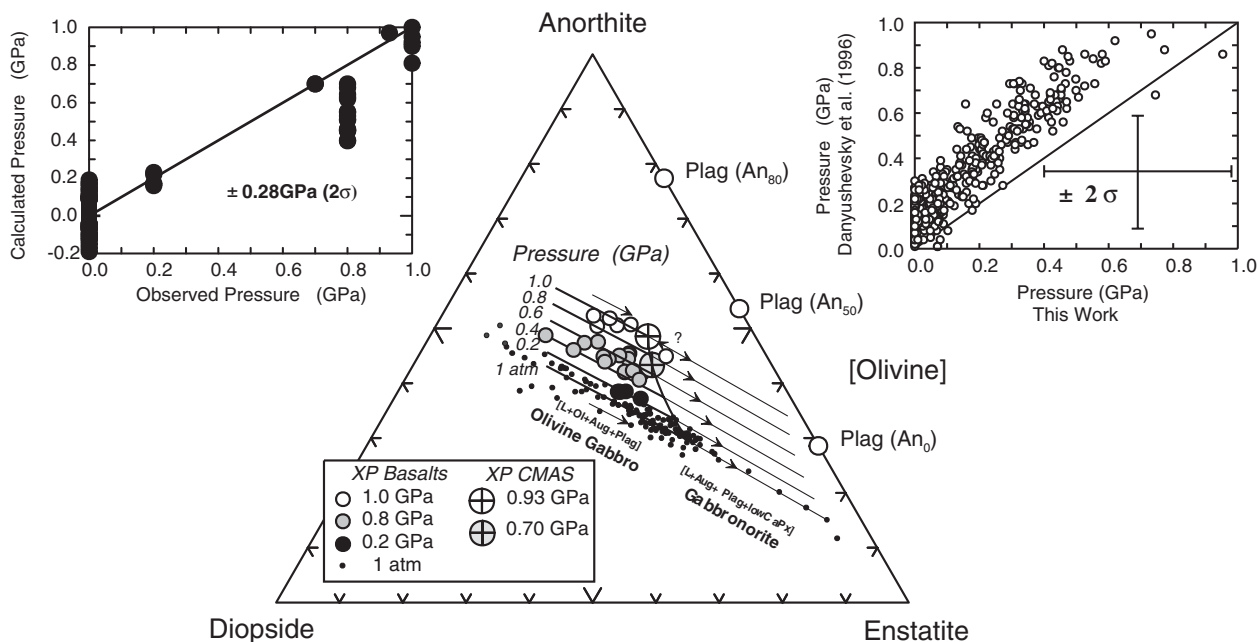
Fig. 1. A projection of experimental data to and from olivine onto the plane Anorthite–Diopside–Enstatite. Method of computing projection co-ordinates and sources of experimental data are given in the text. Left inset shows the pressure calculated for each experimental datum from equation (6) in the text. Right inset compares computed pressures from this work and Danyushevsky *et al.* (1996) on an identical glass database. The effect of pressure is to shift the olivine gabbro cotectic towards Anorthite at the expense of Diopside. The melting of plagioclase lherzolite [L + Ol + low-CaPx + Aug + Plag] is likely to change from a distributary reaction point to a eutectic at pressures greater than about 0·5–0·6 GPa (Longhi, 2002) XP refers to experimental liquid compositions.

GPa. Solutions to equations (4) and (5) are given in Table 1.

For any lava composition that is simultaneously saturated in olivine + plagioclase + augite, the An, Di, En co-ordinates can be computed using equations (1), (2), and (3), and this permits the pressure of equilibration to be computed with the following equation:

$$P = -9{\cdot}1168 + 0{\cdot}2446(0{\cdot}4645\text{En} + \text{An})$$
$$- 0{\cdot}001368(0{\cdot}4645\text{En} + \text{An})^2. \qquad (6)$$

Using this expression, pressures are calculated for liquids in the experimental database and compared with observed pressures. Results are shown as the inset in Fig. 1. Calculated and observed pressures agree to within $\pm0{\cdot}28$ GPa at the 2σ level of confidence.

There are other methods for estimating the pressure of Ol + Plag + Aug crystallization (Weaver & Langmuir, 1990; Danyushevsky *et al.*, 1996; Yang *et al.*, 1996) and these have been extensively reviewed by Michael & Cornell (1998). Pressures estimated for individual MORB using the method of Yang *et al.* (1996) can be as much as 0·3–0·4 GPa higher or lower than those determined with the method of Danyushevsky *et al.* (1996).

The method of Danyushevsky *et al.* (1996) provides calculated pressures that differ from experimental pressures by $\pm0{\cdot}25$ GPa at the 2σ level of confidence, similar to uncertainties reported here. Pressures have been calculated using equation (6) for 423 MORB glass samples in the database of Michael & Cornell (1998); on average, they tend to be 0·16 GPa lower than pressures computed using the method of Danyushevsky *et al.* (1996; see inset in Fig. 1). Nominal pressures at around 1·0 GPa reported from experiments conducted in the piston-cylinder solid medium apparatus can be significantly greater than those conducted with a hydrostatic gas pressure medium apparatus (e.g. Herzberg, 1972; Walter & Presnall, 1994). Pressure uncertainties for piston-cylinder experiments at around 0·7–0·8 GPa in Fig. 1 are expected to be high, but these cannot be evaluated at present.

SOURCES AND TREATMENT OF MORB DATA

MORB glass data used in this work have been mostly obtained from the Petrological Database of the Ocean Floor (PETDB), an NSF (National Science Foundation) funded research project carried by the Lamont–Doherty Earth Observatory and sponsored by RIDGE (Ridge Inter-Disciplinary Global Experiments). The PETDB database is a continuing web-accessed compilation of MORB data that have been obtained from many independent sources (http://petdb.ldeo.columbia.edu), and a description of its structure has

Table 1: Anorthite–Diopside–Enstatite projection co-ordinates

P (GPa)	An	Di	En	Assemblage
0	43·14	35·75	21·11	L + Ol + Plag + Aug
0	29·64	20·18	50·18	L + Ol + Plag + Aug + low-CaPx
0	15·10	5·41	79·50	L + Plag + Aug + low-CaPx
0·2	45·67	34·37	19·97	L + Ol + Plag + Aug
0·2	33·44	20·27	46·29	L + Ol + Plag + Aug + low-CaPx
0·2	18·90	5·50	75·61	L + Plag + Aug + low-CaPx
0·4	48·48	32·75	18·77	L + Ol + Plag + Aug
0·4	37·42	19·99	42·59	L + Ol + Plag + Aug + low-CaPx
0·4	22·88	5·22	71·91	L + Plag + Aug + low-CaPx
0·6	51·44	30·98	17·58	L + Ol + Plag + Aug
0·6	41·40	19·41	39·20	L + Ol + Plag + Aug + low-CaPx
0·6	26·86	4·64	68·52	L + Plag + Aug + low-CaPx
0·8	54·47	29·08	16·45	L + Ol + Plag + Aug
0·8	45·17	18·37	36·46	L + Ol + Plag + Aug + low-CaPx
0·8	30·63	3·60	65·78	L + Plag + Aug + low-CaPx
1·0	57·36	27·20	15·44	L + Ol + Plag + Aug
1·0	48·51	16·99	34·49	L + Ol + Plag + Aug + low-CaPx
1·0	33·97	2·22	63·81	L + Plag + Aug + low-CaPx

Each isobaric co-ordinate is a low- or high-SiO_2 bound on a linear cotectic.

been given by Lehnert *et al.* (2000). A substantial fraction of the glass data in PETDB has been obtained from the Smithsonian Institution (Melson *et al.*, 1977, 2002). Additionally, many MORB data have been compiled from a reference list that includes hundreds of peer-reviewed papers. Unless otherwise stated, these individual contributions will not be cited because they can be directly obtained in PETDB. A large database of MORB glasses for which H_2O analyses are available has been reported by Danyushevsky (2001). For each glass analysis, a computation was made of Fe_2O_3 and FeO using $Fe^{3+}/\sum Fe = 0{\cdot}07$ determined by Christie *et al.* (1986) for 78 MORB glasses. It should be noted that nearly identical projection co-ordinates are obtained when all iron is assumed to occur as FeO. The weight percent analysis was then converted to mole percent, as discussed above, and the An, Di, En projection co-ordinates were computed from equations (1), (2), and (3). Results are discussed below.

REGIONAL VARIATIONS IN PARTIAL CRYSTALLIZATION OF MORB
MORB in projection

Projections have been made of MORB glass compositions from the East Pacific Rise, Juan de Fuca Ridge,

Mid-Atlantic Ridge, Southwest Indian Ridge, and the Mid-Cayman Rise. Results given in Fig. 2 show that there are regional variations in the pressure of partial crystallization that correlate with spreading rate, an observation made also by Michael & Cornell (1998). For fast- and intermediate-spreading centers, more than half of the MORB glass population shows evidence of Ol + Plag + Aug fractionation at crustal pressures, in the 1 atm–0·2 GPa range. In contrast, only a small fraction of MORB glasses from slow-spreading centers display Ol + Plag + Aug fractionation at depths in the crust (Fig. 2). It can be shown that the observations in Fig. 2 are representative of MORB glasses from all other oceanic ridges.

MORB glasses that do not project along low-pressure cotectics defined by liquids in equilibrium with Ol + Plag + Aug at 1 atm–0·2 GPa are subject to several interpretations summarized in Fig. 3. The first possibility is that all fractional crystallization remains at low pressures corresponding to the crust. Let us consider a bulk parental MORB magma that is high in alumina and represented by the cross-in-circle in Fig. 3a. This is a projection of the primary magma estimated by Herzberg & O'Hara (2002) for MORB from the Siqueiros Fracture Zone of the East Pacific Rise (Perfit *et al.*, 1996). Eruption of this magma immediately to the surface would result in the following crystallization sequence
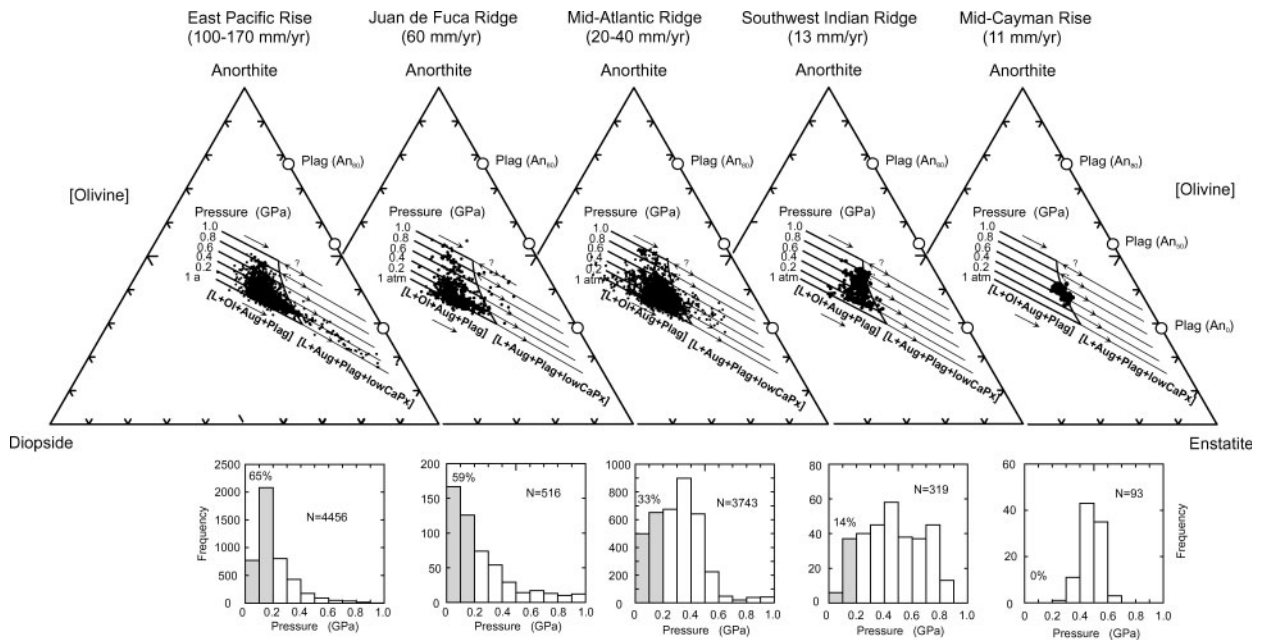
Fig. 2. A projection of MORB glass compositions from five ridges to and from olivine onto the plane Anorthite–Diopside–Enstatite. Histograms below each projection show the percent of glasses that project along the cotectic [L + Ol + Plag + Aug] at 1 atm–0·2 GPa (shaded regions), pressures approximating those of the oceanic crust. N, number of glass analyses in the database. (Note the systematic change in the frequency of glasses that show the characteristics of Ol + Plag + Aug fractionation at low pressures with spreading rate.)
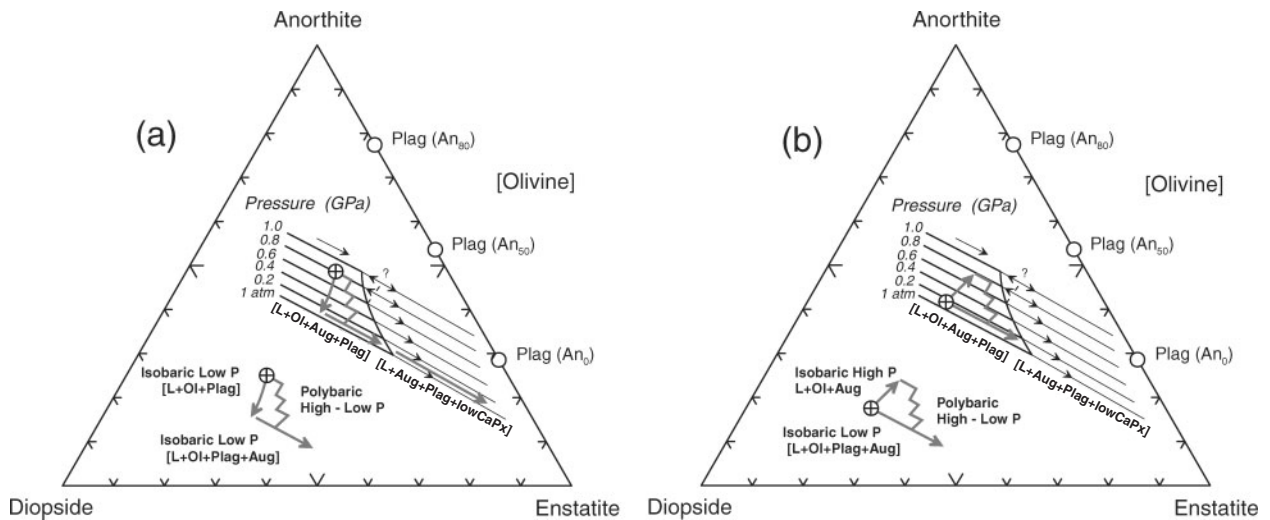

Fig. 3. Interpretations of MORB glasses that project at the cotectic [L + Ol + Plag + Aug] at pressures >0·2 GPa. (a) The standard model showing the crystallization sequence [L + Ol + Plag] → [L + Ol + Plag + Aug] for isobaric and polybaric scenarios; cross-in-circle is primary magma estimated for MORB from the Siqueiros Fracture Zone of the East Pacific Rise (Herzberg & O'Hara, 2002). (b) A model that might describe the less common case of [L + Ol + Aug] → [L + Ol + Plag + Aug]; cross-in-circle is primary magma of picritic basalts from Theistareykir volcano on Iceland, computed from data presented by Slater et al. (2001) using the method of Herzberg & O'Hara (2002).

[L + Ol] → [L + Ol + Plag] → [L + Ol + Plag + Aug]. The crystallization of olivine at the beginning is not observed in Fig. 3a because this is a projection from olivine. However, once plagioclase starts to crystallize with olivine, derivative liquids will move directly away from plagioclase. Aliquots of these liquids produced by variable amounts of Ol + Plag fractionation will erupt to the surface along a locus of points indicated by the arrow. The coincidence of Ol + Plag fractionated glasses with high-pressure Ol + Plag + Aug cotectics has no significance, a point discussed in more detail below. Let us consider now the case of initial fractionation of Ol and

then Ol + Plag + Aug at 0·8 GPa (Fig. 3a). The derivative liquid ascends to 0·6 GPa where it fractionates Ol + Plag and Ol + Plag + Aug; the new derivative liquid ascends to 0·4 GPa where it fractionates more Ol + Plag and Ol + Plag + Aug; eventually it erupts to the surface where it undergoes yet more Ol + Plag fractionation. Such erupted MORB would show the geochemical effects of polybaric Ol + Plag + Aug fractionation but a phenocryst assemblage of olivine + plagioclase. The projection of these polybaric derivative liquids would produce an array of points that represent the integrated product of both Ol + Plag and Ol + Plag + Aug fractionation, and these would project along a locus that is approximately parallel to the An–En side of the projection.

We now consider a parental magma that is higher in CaO and lower in Al_2O_3 and coincident with a low-pressure Ol + Plag + Aug cotectic purely by chance (Fig. 3b). The projected primary magma has been estimated for basalts from Theistareykir volcano on Iceland, computed from data presented by Slater *et al.* (2001) using the method of Herzberg & O'Hara (2002). Although this example might not be representative of MORB, it illustrates the crystallization of possible unmixed instantaneous fractional melts produced from a harzburgite residue with high CaO/Al_2O_3. Isobaric fractionation of the primary magma shown in Fig. 4 at 0·8 GPa would be described by the following crystallization sequence: [L + Ol] → [L + Ol + Aug] → [L + Ol + Aug + Plag]. Polybaric fractional crystallization of derivative liquids from 0·8 GPa to the surface can produce both troctolite and olivine gabbro differentiates (Fig. 3b). Maclennan *et al.* (2001, 2003) reported nodules of both wehrlite (Ol + Aug) and olivine gabbro (Ol + Plag + Aug), and inferred pressures of partial crystallization of 0·34–0·89 GPa. What is important for the present discussion is that the coincidence of glasses that fractionate Ol + Aug with high-pressure Ol + Plag + Aug cotectics has no special significance.

In summary, any glass that projects along a [L + Ol + Plag + Aug] cotectic at pressures above 0·2 GPa is subject to several interpretations. The nominal pressure will be a real pressure if the glass was produced by an increment of Ol + Plag + Aug fractionation. However, the nominal pressure will be an upper bound after an increment of Ol + Plag fractionation, and a lower bound after an increment of Ol + Aug fractionation. A more detailed petrological analysis is required to evaluate whether liquids are saturated in augite, and this is discussed in the following section.

Criteria for augite saturation in MORB

Diagrams that plot MgO vs CaO can be used to evaluate whether a suite of MORB glasses had crystallized augite at some stage [L + Ol + Plag + Aug], and therefore the
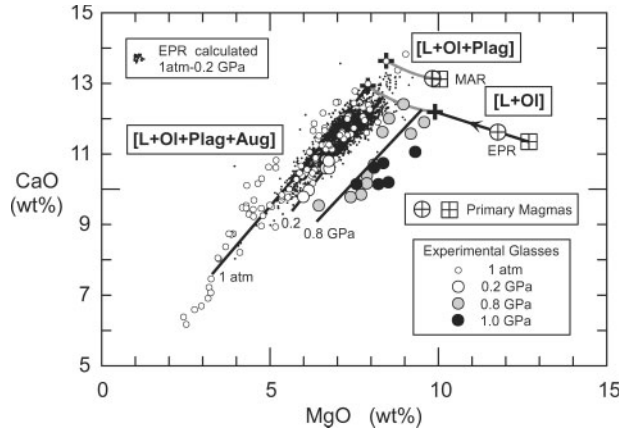

Fig. 4. Variations in CaO vs MgO for liquids that crystallize Ol + Plag and Ol + Plag + Aug. Symbols are defined in the insets, and sources of experimental data are given in the text. Glasses from the East Pacific Rise that are coincident with the [L + Ol + Plag + Aug] cotectic at 1 atm–0·2 GPa are indicated as small black dots, and are very similar to experimental glasses in this pressure range. Cross-in-circle and cross-in-square labelled EPR are primary magmas for MORB glasses from the Siqueiros Fracture Zone (Herzberg & O'Hara, 2002) formed by accumulated fractional melting of fertile and depleted sources, respectively. EPR liquid line of descent for [L + Ol] is calculated from Herzberg & O'Hara (2002). EPR liquid line of descent for [L + Ol + Plag] and [L + Ol + Plag + Aug] at 1 atm is calculated using the PETROLOG software of Danyushevsky (2001), and is similar to other parameterizations (Michael & Chase, 1987; Langmuir *et al.*, 1992; Yang *et al.*, 1996). Some MORB glasses from the Mid-Atlantic Ridge are elevated in CaO compared with glasses from the East Pacific Rise, and they might be examples of fractional melts rather than accumulated fractional melts; the primary magmas labelled as MAR are discussed in the text.

reliability of pressure information obtained from projection. The liquid line of descent (i.e. LLD) for liquids that fractionate Ol then Ol + Plag is shown in Fig. 4 for the primary magmas estimated for MORB from the Siqueiros Fracture Zone of the East Pacific Rise given by Herzberg & O'Hara (2002). Some primitive MORB glasses from the Mid-Atlantic Ridge have somewhat lower FeO_T and higher CaO than comparable glasses from the East Pacific Rise. One possible primary magma from the Mid-Atlantic Ridge shown in Fig. 4 was computed by incremental additions of Ol + Plag to synthetic glass composition P12-28 produced in experiments on basalts from the Oceanographer Fracture Zone (Walker *et al.*, 1979). The calculation was stopped at a liquid composition that displayed internally consistent mass fractions of melting in both projection and FeO–MgO plots (Herzberg & O'Hara, 2002) for accumulated fractional melting of fertile and depleted peridotite. It is possible that this primary magma composition might not be representative of the Mid-Atlantic Ridge, but it is provided in order to consider the variability in CaO contents that might arise from source heterogeneities or incomplete mixing of instantaneous fractional melts. However, the range of liquids fractionated from

Ol + Plag is very similar to that offered by Langmuir *et al.* (1992) for MORB from the FAMOUS–AMAR region.

CaO increases marginally during Ol and Ol + Plag fractionation, then decreases substantially during Ol + Plag + Aug fractionation. The LLD shown for Ol + Plag and Ol + Plag + Aug fractionation at 1 atm in Fig. 4 is calculated according to the program PETROLOG (Danyushevsky, 2001), and the results are very similar to other parameterizations (Michael & Chase, 1987; Langmuir *et al.*, 1992; Yang *et al.*, 1996). For Ol + Plag + Aug fractionation at 1 atm, the calculated LLD is very similar to experimental glass compositions and to EPR glasses in Fig. 2 that display pressures between 1 atm and 0·2 GPa (Fig. 4). Low-K_2O experimental glass compositions appropriate for normal MORB at 0·2–1·0 GPa reveal a systematic shift in the LLD to higher MgO compositions (Bender *et al.*, 1978; Falloon & Green, 1987; Bartels *et al.*, 1991; Grove *et al.* 1992). Linear regressions of experimental data at 0·2 and 0·8 GPa given in Fig. 4 are similar to the calculated LLD of Langmuir *et al.* (1992) and Yang *et al.* (1996).

The CaO and MgO contents of MORB glasses from the East Pacific Rise, Mid-Atlantic Ridge and the Mid-Cayman Rise are now shown in Fig. 5. For clarity, the data for each ridge are divided into two populations, based on pressures of Ol + Plag + Aug inferred from projection (Fig. 2) and calculated with equation (6). One group displays pressures in the 1 atm–0·6 GPa range, the other pressures in excess of 0·6 GPa. Figure 5 shows that there is very good agreement in pressures inferred from projection and those based on CaO–MgO systematics. This agreement is not perfect because liquids with variable alkali contents can display considerable variability in MgO, an effect that is considered in the projection code. This is manifest in some natural MORB glasses that display higher pressures in projection than in plots of CaO–MgO.

MORB glasses from the East Pacific Rise that are coincident with the Ol + Plag + Aug cotectic at 1 atm–0·2 GPa exhibit the depletion in CaO expected from augite fractionation (Fig. 4). Depletion in CaO occurs also for glasses in the high-pressure population, indicating Ol + Plag + Aug fractionation in excess of 0·6 GPa (Fig. 5a). However, EPR glasses with the highest CaO contents are also similar to liquids that are expected to fractionate Ol + Plag. This observation illustrates the point raised above that the coincidence of Ol + Plag fractionated glasses with high-pressure Ol + Plag + Aug cotectics in projection has no significance. In addition to glasses from the EPR and MAR, MORB glasses from the Lamont Seamounts (Danyushevsky *et al.*, 2000) and the Galapagos Spreading Center also display prominent Ol + Plag fractionation. Liquids from many ridges that can crystallize Ol + Plag contain CaO in excess of those defined by
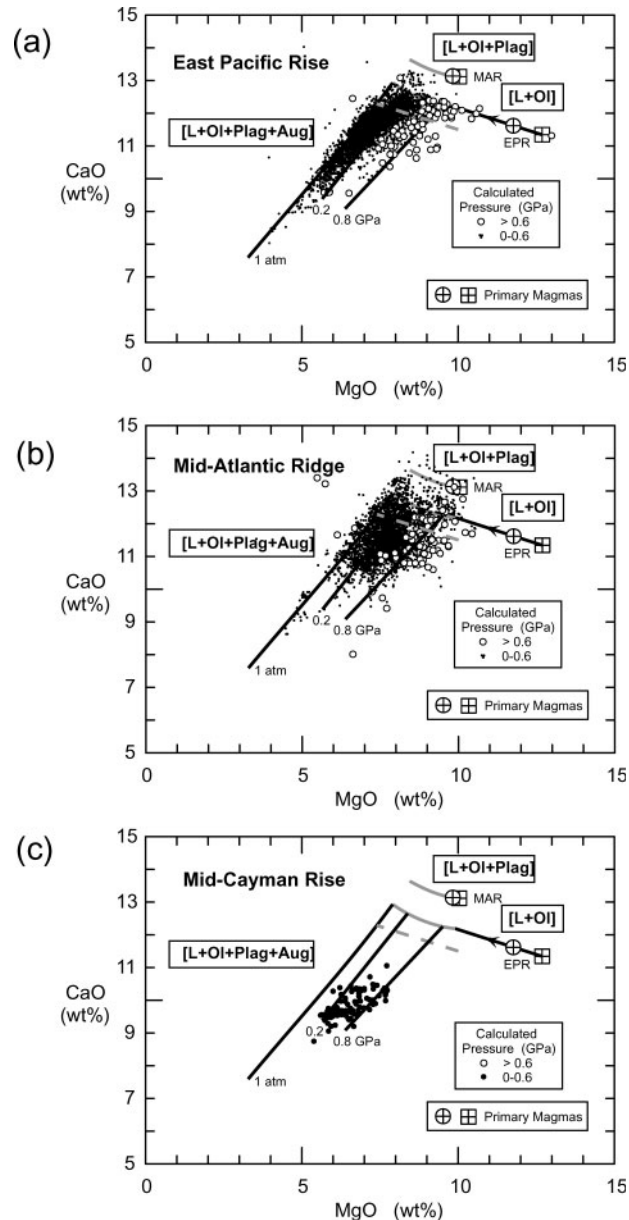

Fig. 5. Variations in CaO vs MgO for glasses from the East Pacific Rise, the Mid-Atlantic Ridge, and the Mid-Cayman Rise. The pressure at which each glass analysis was assumed to crystallize Ol + Plag + Aug was computed from equation (6) in the text. Liquid lines of descent for [L + Ol] → [L + Ol + Plag] → [L + Ol + Plag + Aug] are from Fig. 4. The dashed gray line represents a likely lower bound on the CaO contents of MORB glasses that crystallize Ol + Plag, and can be described by the equation CaO = 0·3MgO + 14·5.

the dashed gray lines in Fig. 5, which can be described by the equation CaO = −0·3MgO + 14·5. This equation will be used below to filter out glasses that fractionated Ol + Plag and Ol + Plag + Aug on the high-CaO and low-CaO side of the gray line, respectively. The filter might, however, miss glasses that had experienced

Ol + Plag fractionation from low-CaO liquids that experienced Ol + Plag + Aug fractionation at high pressures as discussed for Fig. 3a [see also discussion by Langmuir *et al.* (1992)].

It was shown by projection that there is a systematic decrease in the number of glasses that record the characteristics of Ol + Plag + Aug fractionation at low pressures with a reduction in spreading rate (Fig. 2). This is seen also in plots of CaO–MgO (Fig. 5a–c). Most MORB from the Mid-Atlantic Ridge and the Mid-Cayman Rise display prominent fractionation of Ol + Plag + Aug above 0·2 GPa in both projection (Fig. 2) and CaO–MgO space (Fig. 5b and c). Pressures of partial crystallization of glasses from the Mid-Cayman Rise were suggested to be as high as 0·5–0·6 GPa (Grove *et al.*, 1992; Elthon *et al.*, 1995), in good agreement with those inferred from projection and plots of CaO–MgO.

Effects of H_2O on estimated pressures of partial crystallization

Although there are regional variations in the H_2O content of MORB (Michael, 1995; Danyushevsky *et al.*, 2000), these are not generally correlated with spreading rate. Therefore, the systematic variations in the pressure of partial crystallization shown in Fig. 2 are not likely to be artifacts of H_2O. However, it is worth exploring how H_2O variability in MORB will affect pressures inferred from projections. Experimental studies show that addition of H_2O can suppress plagioclase crystallization relative to olivine and clinopyroxene (Yoder, 1965; Dixon Spulber & Rutherford, 1983; Gaetani *et al.*, 1993; Sisson & Grove, 1993). Petrological models describe how this can result in derivative liquids with higher Al_2O_3 at a given MgO content (Michael & Chase, 1987; Danyushevsky, 2001; Asimow & Langmuir, 2003). Addition of H_2O will shift the projected cotectics away from augite and towards plagioclase; however, the data of Sisson & Grove (1993) show that that large H_2O contents are required to produce a significant effect.

Plots of 682 MORB glasses for which both major element and H_2O contents have been measured (Danyushevsky, 2001) are shown in Fig. 6. These data have been divided into two populations, with glasses that have more than or less than 0·2% H_2O. Many glasses in the dry group with <0·2% H_2O have CaO >12%, and are likely to be differentiates of Ol + Plag fractionation; other glasses in the dry group with lower CaO contents are likely to be differentiates of Ol + Plag + Aug fractionation. MORB glasses with H_2O >0·2% generally contain CaO <12% (Fig. 6a), consistent with compatible element behavior during partial crystallization of Ol + Plag + Aug. Glasses in both the wet and dry populations exhibit partial crystallization of Ol + Plag + Aug at pressures that range from 1 atm to >0·8 GPa. Wet

glasses do not display higher pressures in either CaO–MgO space (Fig. 6a) or projection (Fig. 6b). There is no correlation between H_2O content and pressure of Ol + Plag + Aug fractionation as shown also in Fig. 7 for glasses that have been filtered to exclude those that crystallized Ol + Plag; the same holds true for the entire unfiltered database.

Magma mixing

Several workers have noted possible ambiguities in pressure interpretations that might arise from magma mixing (Grove *et al.*, 1992; Michael & Cornell, 1998). Magma mixing in this context refers to the mixing of magmas that are part of a liquid line of descent at low pressures appropriate to the crust (e.g. Langmuir, 1989). For example, inspection of CaO–MgO for the East Pacific Rise in Fig. 5a shows that glasses that exhibit partial crystallization of Ol + Plag + Aug at pressures >0·6 GPa might be explained by the mixing of low-pressure primitive and differentiated magmas with high and low MgO contents, respectively. However, this mixing explanation might be more problematic for glasses from the Mid-Atlantic Ridge that have high MgO and low CaO and display partial crystallization at >0·6 GPa. Figure 5b shows that this glass population cannot be a mixture of end-members defined by primary magmas with about 10% MgO and differentiates at 1 atm–0·2 GPa. Additionally, glasses from slow-spreading centers generally exhibit higher pressures of crystallization than do glasses from faster-spreading ridges, and it is not clear why magma mixing would correlate with spreading rate.

Fracture zones and spreading rate

For fast- and intermediate-spreading centers, more than 50% of MORB glass compositions show evidence of Ol + Plag + Aug fractionation at crustal pressures (i.e. 1 atm–0·2 GPa), the remainder showing fractionation at pressures in the 0·2–1·0 GPa range (Fig. 2). Shallow depth olivine gabbro fractionation is prominent among MORB from the East Pacific Rise and Juan de Fuca Ridge (Fig. 2), in addition to the Galapagos Spreading Center. These results are consistent with models of layered gabbro formation (i.e. layer 3) in steady-state magma chambers below fast-spreading ridges (e.g. Sleep, 1975; Detrick *et al.*, 1987; Dick, 1989; Nicolas, 1989; Hekinian *et al.*, 1993; Dick *et al.*, 2000). They are also consistent with seismic evidence for shallow magma chambers beneath the East Pacific Rise (Detrick *et al.*, 1987; Scheirer *et al.*, 1998). A more detailed view is given in Fig. 8 of computed pressures for MORB glasses from the East Pacific Rise between 5 and 15°N. The database of 3758 glass analyses has been filtered to exclude samples that had fractionated Ol + Plag as discussed above; these
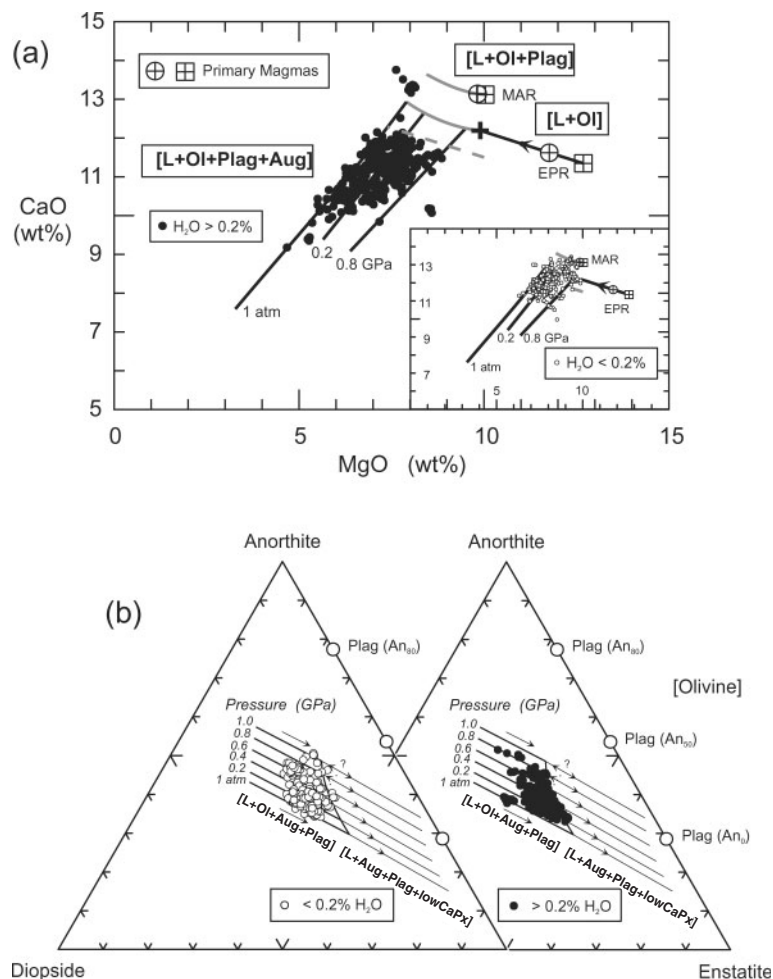
Fig. 6. A database of 682 MORB glasses for which H_2O contents have been measured (Danyushevsky, 2001). ●, H_2O >0·2% (0·2–0·9%); ○, H_2O <0·2%. (a) Variations in CaO vs MgO; (b) glasses projected to and from olivine onto the plane Anorthite–Diopside–Enstatite.

are glasses with CaO $> -0·3$MgO $+ 14·5$, and they represent 15% of the total population. Although pressures are mostly low, MORB glasses from the Siqueiros Fracture Zone display both the highest pressures and a variability that spans the 1 atm–0·8 GPa range. In general, the pressure of partial crystallization of Ol + Plag + Aug correlates with proximity to ridge segment centers or terminations (Fig. 8), similar to the variability reported by Dmitriev (1998). Terminations are defined as fracture zones, overlapping spreading centers (i.e. OSC; Macdonald et al., 1988), and deviations from axial linearity (devals; Langmuir et al. 1986). There is a cluster of OSCs and devals between 11° and 13°N, and these are associated with both low and high pressures of crystallization. In contrast, MORB glasses from unsegmented ridges or segment centers display the low pressures that are more characteristic of those of the crust. Glasses from the Clipperton Fracture Zone also display uniformly low pressures; the lack of high-pressure MORB will be discussed below.

A detailed view of slow-spreading ridges in the Atlantic from the equator to north of Iceland is provided in Fig. 9. Most glasses display prominent Ol + Plag + Aug fractionation at depths in the mantle (Figs 2 and 9), in good agreement with previous estimates (Tormey et al., 1987; Grove et al., 1992; Dmitriev, 1998; Michael & Cornell, 1998). Glasses have been filtered to exclude those that fractionated Ol + Plag as discussed above, and represent 27% of the total glass population of 4671 analyses. As with the East Pacific Rise, higher pressures are typically associated with fracture zones. Filtering the database for samples with CaO that is 1% lower would exclude 72% of the total glass population as possible differentiates of Ol + Plag fractionation; however, the remaining glasses still show that the pressure of crystallization is strongly correlated with proximity to fracture zones. The greater frequency of high pressures found at slow-spreading centers compared with fast-spreading centers might be a reflection of the rougher and more heavily faulted topography (Macdonald, 1982).
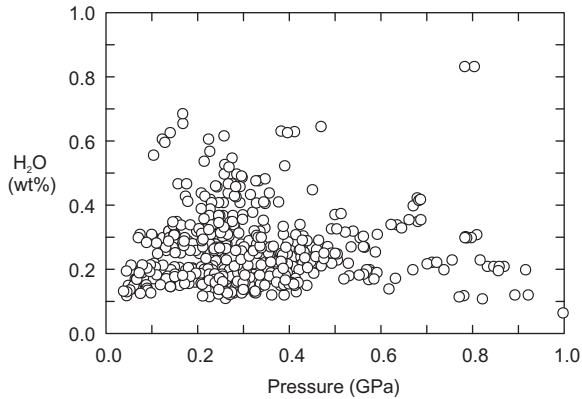
Fig. 7. Variations in H_2O content of 682 MORB glasses from Danyushevsky (2001) with calculated pressure of Ol + Plag + Aug crystallization from equation (6) in the text. Glasses have been filtered to exclude samples that had fractionated Ol + Plag. The poor correlation should be noted.

Fig. 8. Pressures of Ol + Plag + Aug fractionation for MORB from the East Pacific Rise between 5°N and 15°N calculated using equation (6). The Siqueiros and Clipperton Fracture Zones are indicated; all others are that are not labelled are overlapping spreading centers and deviations from axial linearity from Langmuir *et al.* (1986). It should be noted that the highest pressures are usually observed for MORB associated with ridge segment terminations, especially the Siqueiros Fracture Zone and the group of terminations at 11–13°N. Glasses for which Ol + Plag fractionation was likely have been filtered out as discussed in the text; these have CaO > −0·3MgO + 14·5. If this window of filtering is widened further by lowering CaO another 1%, then 65% of the total glass population would be excluded, and it would have the undesirable effect of excluding glasses that had fractionated Ol + Plag + Aug. Nevertheless, it can be shown that there is no change in the correlation of high pressures of crystallization with ridge segment terminations.

MORB glasses from very slow-spreading centers such as the Mid-Cayman Rise consistently display pressures of crystallization that correspond to mantle depths (Figs 2 and 5c). This might explain why lower-crustal gabbros at the Southwest Indian Ridge are Fe-rich (Dick *et al.*, 2000; Coogan *et al.*, 2001). The Southwest Indian Ridge near the Atlantis II Fracture Zone exhibits bathymetric offsets over ridge length scales of some 10 km or less. Magmas from ridge segment terminations and centers might intermingle as separate lava flows. Should mixing occur, mantle pressures computed for MORB at slow-spreading centers might be over-represented. Nevertheless, these results indicate that partial crystallization can take place within the mantle as suggested by Coogan *et al.* (2001) and above the top of the melting column, which White *et al.* (2001) placed at about 20 km below the surface for very slow-spreading centers.

MORB glasses from the Reykjanes Ridge provide an important exception to the observation in Fig. 2 that slow-spreading centers are associated with high pressures of partial crystallization. The Reykjanes Ridge has a spreading rate of only 20 mm/yr, but erupts MORB with low crustal pressures that are more characteristic of the East Pacific Rise than the Mid-Atlantic Ridge (Fig. 9). The low pressures for the Reykjanes Ridge are in good agreement with previous estimates (Grove *et al.*, 1992; Dmitriev, 1998; Michael & Cornell, 1998) and with crustal magma chambers that have been seismically imaged on the Reykjanes Ridge at 57·75°N (Navin *et al.*, 1998). However, unlike most of the Mid-Atlantic Ridge, the Reykjanes Ridge overlies a thickened crust that is not segmented.

There is a general decrease in crustal thickness and an increase in axial depth as a transform fault is approached (White *et al.*, 1984, 2001; Shen & Forsyth, 1992; Bown & White, 1994; Muller *et al.*,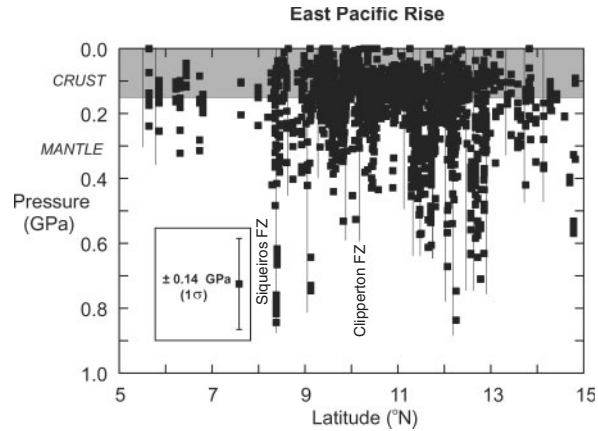 1999, 2000), features that can be subdued at faster-spreading ridges. It has been suggested that transform faults increase opportunities for conductive cooling to penetrate deep into the mantle (Shen & Forsyth, 1992, 1995). This interpretation would predict partial crystallization of MORB at depth, in good agreement with the observed association of fracture zones and high pressures of partial crystallization shown in Figs 8 and 9.

There is now a considerable body of geochemical evidence that hot mantle from the Icelandic plume is being channeled into the Reykjanes Ridge (Sun *et al.*, 1975; Taylor *et al.*, 1997; Kempton *et al.*, 2000; Murton *et al.*, 2002). The mantle is not sufficiently cold for partial crystallization to occur, and pressures are mostly low and correspond to those in the crust (Fig. 9). Similarly, MORB along the Mid-Atlantic Ridge near the Azores platform display low pressures of crystallization appropriate to the crust, but both crust and mantle pressures at adjacent fracture zones (Fig. 9).

LITHOLOGICALLY HETEROGENEOUS MANTLE

Pressures of Ol + Plag + Aug partial crystallization range from 1 atm to 1·0 GPa for slow- and fast-spreading ridges. Pressures corresponding to upper-mantle depths are
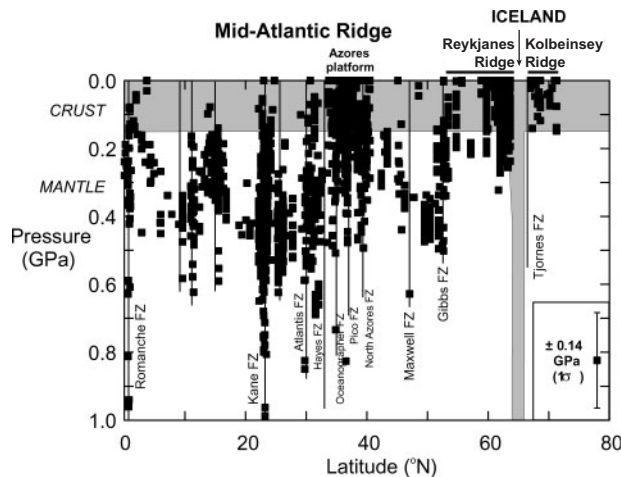
Fig. 9. Pressures of Ol + Plag + Aug fractionation for MORB from the Mid-Atlantic, Reykjanes, and Kolbeinsey Ridges calculated using equation (6). Glasses for which Ol + Plag fractionation was likely have been filtered out as discussed in the text. It should be noted that the highest pressures are usually observed for MORB associated with fracture zones. This figure is very similar to one shown by Dmitriev (1998), who computed pressures using a modified method of Danyushevsky *et al.* (1996).

consistent with observations of veins, dikes, and segregations of gabbro and dunite within residual host peridotites, direct evidence of melt transport and partial crystallization in the mantle (Dick, 1989; Nicolas, 1989; Ceuleneer & Rabinowicz, 1992; Hekinian *et al.*, 1993; Kelemen *et al.*, 1995, 2000; Dick & Natland, 1996).

Veins of pyroxenite and eclogite are often hosted by peridotites in tectonic slices of alpine peridotite massifs throughout Europe and elsewhere (e.g. Carswell, 1968; Kornprobst, 1969; Obata, 1980). In some models, cumulate and residuum interpretations have been applied to whole-rock Lu/Hf and Sm/Nd fractionations (Blichert-Toft *et al.*, 1999). A frequently cited model is that they are residues that were left by the melting of subducted oceanic crust (Allègre & Turcotte, 1986; Blichert-Toft *et al.*, 1999). Substantial stretching and thinning is required to produce centimeter-scale pyroxenite layers from 6 km of oceanic crust (Allègre & Turcotte, 1986). However, the stretching requirement is considerably relaxed or eliminated if some eclogite layers formed by recrystallization of peridotite-hosted centimeter-scale gabbro veins and dikes in abyssal peridotites and ophiolites.

DEPTHS OF MORB PARTIAL MELTING AND PARTIAL CRYSTALLIZATION

The partial melting regime is bounded at the bottom and the top by the depths at which partial melting begins and terminates, respectively. The melting regime is expected to be roughly triangular in shape (Ahern & Turcotte, 1979; McKenzie & Bickle, 1988; Langmuir *et al.*, 1992; Forsyth *et al.*, 1998). Forward petrological models place the depth of final melting, in the center of the upflow, at or near the base of the crust or in the mantle (Klein & Langmuir, 1987; Grove *et al.*, 1992; Shen & Forsyth, 1992, 1995; Forsyth, 1993; Niu, 1997; Asimow *et al.*, 2001; White *et al.*, 2001). The observation of low Rayleigh wave velocities in the depth range 15–70 km on the East Pacific Rise at 17°S has been interpreted as indicating the presence of melt within the melting regime (Forsyth *et al.*, 1998). A depth of 15 km ($\sim$0·4 GPa) for the top of the melting regime compares with pressures of crystallization of Ol + Plag + Aug for MORB glasses from this region that is limited to 1 atm–0·2 GPa. Unfortunately, this work cannot constrain the depth to the top of the melting regime below ridge segment centers that record crustal pressures of crystallization. Magma with a prior record of partial crystallization in the mantle may be modified by re-equilibration during partial crystallization in the crust. However, pressures of crystallization span the 1 atm–0·7 GPa range for glasses from the Garrett Fracture Zone to the north at about 13·5°S (i.e. pressures for glasses that have been filtered to exclude those that exhibit Ol + Plag fractionation), indicating considerable 'topography' to the top of the melting regime.

A generic model that provides a simplified geological context for interpreting the pressures of MORB crystallization is given in Fig. 10. It does not show variations in the depth to the top of the melting regime that might depend on spreading rate (Shen & Forsyth, 1992). It focuses instead on different possible delivery routes of MORB to the surface. In particular, opportunities for tapping partial crystallization products at high pressures are likely to increase if the region consists of a system of branching melt conduits. This is an adaptation of the inverted 'bush' structure of Kelemen *et al.* (2000), who proposed it as a model for melt channels within which dunite is precipitated in the melting regime. A similar structure may also apply to the distribution of olivine gabbro veins and segregations in the region dominated by partial crystallization (e.g. Dick & Natland, 1996). At fracture zone locations, MORB may travel in melt conduits that pass through the crust and terminate at the surface without being modified by Ol + Plag + Aug crystallization in shallow magma chambers. Conversely, melt conduits deliver MORB directly into crustal magma chambers at ridge midpoints. Any record of deep crystallization in the mantle may be filtered out by fractional crystallization in the crust, a process that is likely to be most important at fast-spreading ridges.

Magmas may flow laterally in the crust from segment midpoints to terminations (Dick, 1989; Dick *et al.*, 2000; Abelson *et al.*, 2001; White *et al.*, 2001). MORB from the Clipperton Fracture Zone may be an example because
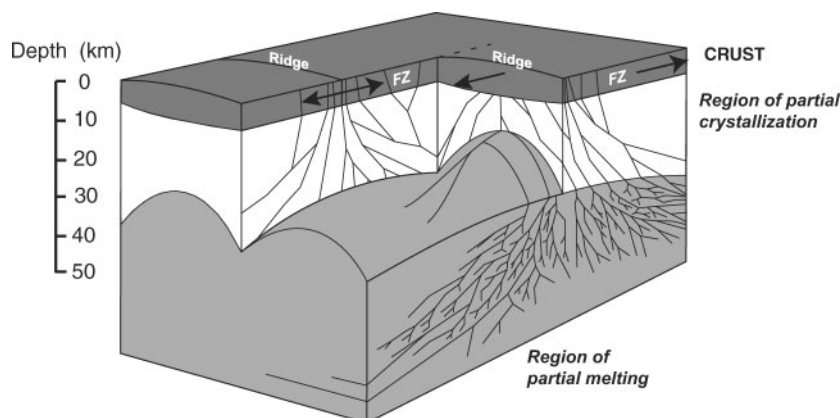
Fig. 10. A model of partial melting and crystallization below oceanic ridges. Branches depict conduits of magma transport located in both partial melting and crystallization regions, adapted from Kelemen *et al.* (2000). Branches end at the base of the crust at a ridge segment center, but they end at the surface at a fracture zone. Partial crystallization occurs in both crust and mantle.

they display compositions that are similar to MORB equilibrated in crustal magma chambers. There may be complex cases where magmas leak out of a magma chamber and into an adjacent fracture zone where they mix with unrelated magmas from deep in the mantle. In this situation, crustal pressures might be underrepresented in MORB glasses owing to the mixing of magmas from low and high pressures.

DISCUSSION

Pressures at which partial crystallization occurs for MORB have been examined with a new petrological method that is based on a parameterization of experimental data in the form of projections. Application to a global glass database shows that Ol + Plag + Aug partial crystallization ranges from 1 atm to 1·0 GPa, and there are regional variations that generally correlate with spreading rate. Pressures corresponding to upper-mantle depths are consistent with observations of veins, dikes, and segregations of gabbro and dunite within residual host peridotites (e.g. Dick & Natland, 1996). Results reported here are in good agreement with previous petrological estimates (Grove *et al.*, 1992; Elthon *et al.*, 1995; Dmitriev, 1998; Michael & Cornell, 1998), and in this sense they are not original. However, this paper provides an independent assessment of the pressures of partial crystallization, and the results have a number of implications for understanding MORB partial melting, the origin of heterogeneous mantle, and the structure of the lithosphere below oceanic ridges.

Michael & Cornell (1998) suggested that variations in magma flux and advected heat might explain the correlations of pressure of crystallization and spreading rate. Compared with fast-spreading centers, there is a lower magma supply and amount of heat that is transported at slower-spreading centers; both crust and mantle are cooler, and partial crystallization occurs at deeper levels (Michael & Cornell, 1998). Spreading rate controls the loss of heat to the surface; at slow spreading rates there is more time for conductive cooling to penetrate the mantle (Shen & Forsyth, 1992, 1995; Bown & White, 1994; White *et al.*, 2001). It was further suggested that the mantle is colder at adjacent transform faults owing to enhanced conductive heat loss (Shen & Forsyth, 1992, 1995). Indeed, Dmitriev (1998) demonstrated that there are important variations in the pressure of partial crystallization of MORB that correlate with ridge segmentation, an observation that is also made in the present work. MORB from fast-spreading centers display partial crystallization in the crust at ridge segment centers and in both mantle and crust at ridge terminations (Fig. 8). Deep melt conduits might deliver high-pressure MORB directly to the surface without being modified by Ol + Plag + Aug crystallization in shallow magma chambers. MORB from slow-spreading centers display prominent partial crystallization in the mantle, consistent with models of enhanced conductive cooling of the lithosphere and the greater abundance of fracture zones through which they pass (Fig. 9).

Glasses from the slow-spreading and unsegmented Reykjanes Ridge illustrate the importance of the intrinsic temperature of the mantle. Unlike the Mid-Atlantic Ridge, the mantle source for Reykjanes MORB is intrinsically hot because it is being fed by horizontal channeling from the Icelandic plume; the mantle is not sufficiently cold for partial crystallization to occur there. Consequently, Reykjanes MORB exhibits prominent crystallization at low pressures that correspond to those

in the crust. Similarly, MORB along the Mid-Atlantic Ridge near the Azores platform display low pressures of crystallization appropriate to the crust, but both crust and mantle pressures at adjacent fracture zones (Fig. 9). Although this analysis has been confined to MORB, it can be demonstrated that basalts from Hawaii and the Ontong Java Plateau also display low pressure of partial crystallization appropriate to magma chambers in the crust. In general, magmas that pass through cold mantle experience some partial crystallization, whereas magmas that move through hot mantle may be comparatively unaffected.

Estimated pressures of partial crystallization indicate that the top of the partial melting region is deeper than about 20–35 km below slow-spreading centers and ridge terminations at fast-spreading centers. Unfortunately, the depth to the top of the melting column below ridge segment centers at fast-spreading ridges cannot be constrained with the method developed here owing to substantial partial crystallization in the crust. Distinguishing the products of partial melting and partial crystallization in MORB petrogenesis remains a challenge long after it was first recognized as a problem (O'Hara, 1968a).

ACKNOWLEDGEMENTS

REFERENCES

Abelson, M., Baer, G. & Agnon, A. (2001). Evidence from gabbro of the Troodos ophiolite for lateral magma transport along a slow-spreading mid-ocean ridge. *Nature* **409**, 72–75.

Ahern, J. L. & Turcotte, D. L. (1970). Magma migration beneath an ocean ridge. *Earth and Planetary Science Letters* **45**, 115–122.

Allègre, C. J. & Turcotte, D. L. (1986). Implications of a two-component marble-cake mantle. *Nature* **323**, 123–127.

Asimow, P. D. & Langmuir, C. H. (2003). The importance of water to oceanic mantle melting regimes. *Nature* **421**, 815–820.

Asimow, P. D., Hirschmann, M. M. & Stolper, E. M. (2001). Calculation of peridotite partial melting from thermodynamic models of minerals and melts, IV. Adiabatic decompression and the composition and mean properties of mid-ocean ridge basalts. *Journal of Petrology* **42**, 963–998.

Baker, D. R. & Eggler, D. H. (1987). Compositions of anhydrous and hydrous melts coexisting with plagioclase, augite, and olivine or low-Ca pyroxene from 1 atm to 8 kbar: application to the Aleutian volcanic center of Atka. *American Mineralogist* **72**, 12–28.

Bartels, K. S., Kinzler, R. J. & Grove, T. L. (1991). High pressure phase relations of primitive high-alumina basalts from Medicine Lake volcano, northern California. *Contributions to Mineralogy and Petrology* **108**, 253–270.

Bender, J. F., Hodges, F. N. & Bence, A. E. (1978). Petrogenesis of basalts from the project FAMOUS area: experimental study from 0 to 15 kbars. *Earth and Planetary Science Letters* **41**, 277–302.

Biggar, G. M. (1984). The composition of diopside solid solutions and of liquids, in equilibrium with forsterite, plagioclase and liquid in the system Na_2O–CaO–MgO–Al_2O_3–SiO_2 and in remelted rocks from 1 bar to 12 kbar. *Mineralogical Magazine* **48**, 481–494.

Biggar, G. M. & Humphries, D. J. (1981). The plagioclase, forsterite, diopside, liquid equilibrium in the system CaO–Na_2O–MgO–Al_2O_3–SiO_2. *Mineralogical Magazine* **44**, 309–314.

Blichert-Toft, J., Albarède, F. & Kornprobst, J. (1999). Lu–Hf isotope systematics of garnet pyroxenites from Beni Bousera, Morocco: implications for basalt origin. *Science* **283**, 1303–1306.

Bown, J. W. & White, R. S. (1994). Variation with spreading rate of oceanic crustal thickness and geochemistry. *Earth and Planetary Science Letters* **121**, 435–449.

Bryan, W. B. (1979). Regional variation and petrogenesis of basalt glasses from the FAMOUS area, Mid-Atlantic Ridge. *Journal of Petrology* **20**, 293–325.

Carswell, D. A. (1968). Picritic magma–residual dunite relationships in garnet peridotite at Kalskaret near Tafjord, South Norway. *Contributions to Mineralogy and Petrology* **19**, 97–124.

Ceuleneer, G. & Rabinowicz, M. (1992). Mantle flow and melt migration beneath oceanic ridges: models derived from observations in ophiolites. In: Phipps Morgan, J., Blackman, D. K. & Sinton, J. M. (eds) *Mantle Flow and Melt Generation at Mid-Ocean Ridges. Geophysical Monograph, American Geophysical Union* **71**, 123–154.

Christie, D. M., Carmichael, I. S. E. & Langmuir, C. H. (1986). Oxidation states of mid-ocean ridge basalt glasses. *Earth and Planetary Science Letters* **79**, 397–411.

Coogan, L. A., MacLeod, C. J., Dick, H. J. B., Edwards, S. J., Kvassnes, A., Natland, J. H., Robinson, P. T., Thompson, G. & O'Hara, M. J. (2001). Whole-rock geochemistry of gabbros from the Southwest Indian Ridge: constraints on geochemical fractionations between the upper and lower oceanic crust and magma chamber processes at (very) slow-spreading ridges. *Chemical Geology* **178**, 1–22.

Danyushevsky, L. V. (2001). The effect of small amounts of H_2O on crystallisation of mid-ocean ridge and backarc basin magmas. *Journal of Volcanology and Geothermal Research* **110**, 265–280.

Danyushevsky, L. V., Sobolev, A. V. & Dmitriev, L. V. (1996). Estimation of the pressure of crystallization and H_2O content of MORB glasses: calibration of an empirical technique. *Mineralogy and Petrology* **57**, 185–204.

Danyushevsky, L. V., Eggins, S. M., Falloon, T. J. & Christie, D. M. (2000). H_2O abundance in depleted to moderately enriched mid-ocean ridge magmas; Part I: incompatible behaviour, implications for mantle storage, and origin of regional variations. *Journal of Petrology* **41**, 1329–1364.

Detrick, R. S., Buhl, P., Vera, E., Mutter, J., Orcutt, J., Madsen, J. & Brocher, T. (1987). Multi-channel seismic imaging of a crustal magma chamber along the East Pacific Rise. *Nature* **326**, 35–41.

Dick, H. J. B. (1989). Abyssal peridotites, very slow spreading ridges and ocean ridge magmatism. In: Saunders, A. D. & Norry, M. J.

(eds) *Magmatism in the Ocean Basins. Geological Society, London, Special Publications* **42**, 71–105.

Dick, H. J. B. & Natland, J. H. (1996). Late-stage melt evolution and transport in the shallow mantle beneath the East Pacific Rise. In: Mével, C., Allan, K. M. & Meyer, P. S. (eds) *Proceedings of the Ocean Drilling Program, Scientific Results, 147.* College Station, TX: Ocean Drilling Program, pp. 103–134.

Dick, H. J. B., Natland, J. H., Alt, J. C., *et al.* (2000). A long in situ section of the lower oceanic crust: Leg 176 drilling at the Southwest Indian Ridge. *Earth and Planetary Science Letters* **179**, 31–51.

Dixon Spulber, S. & Rutherford, M. J. (1983). The origin of rhyolite and plagiogranite in oceanic crust: an experimental study. *Journal of Petrology* **24**, 1–25.

Dmitriev, L. V. (1998). Chemical variability of mid-ocean ridge basalts as a function of the geodynamic setting of their formation. *Petrology* **6**, 314–334.

Dungan, M. A. & Rhodes, J. M. (1978). Residual glasses and melt inclusions in basalts from DSDP Legs 45 and 46: evidence for magma mixing. *Contributions to Mineralogy and Petrology* **67**, 417–431.

Elthon, D., Ross, D. K. & Meen, J. K. (1995). Compositional variations of basaltic glasses from the Mid-Cayman Rise spreading center. *Journal of Geophysical Research* **100**, 12497–12512.

Falloon, T. J. & Green, D. H. (1987). Anhydrous partial melting of MORB pyrolite and other peridotite compositions at 10 kbar: implications for the origin of primitive MORB glasses. *Mineralogy and Petrology* **37**, 181–219.

Fisk, M. R., Schilling, J.-G. & Sigurdsson, H. (1980). An experimental investigation of Iceland and Reykjanes Ridge tholeiites: I. Phase relations. *Contributions to Mineralogy and Petrology* **74**, 361–374.

Forsyth, D. W. (1993). Crustal thickness and the average depth and degree of melting in fractional melting models of passive flow beneath mid-ocean ridges. *Journal of Geophysical Research* **98**, 16073–16079.

Forsyth, D. W., Scheirer, D. S., Webb, S. C., *et al.* (1998). Imaging the deep seismic structure beneath a mid-ocean ridge: the MELT experiment. *Science* **280**, 1215–1218.

Francis, D. (1980). The pyroxene paradox in MORB glasses—a signature of picritic parental magmas? *Nature* **319**, 586–588.

Fujii, T. & Bougault, H. (1983). Melting relations of a magnesian abyssal tholeiite and the origin of MORBs. *Earth and Planetary Science Letters* **62**, 283–295.

Gaetani, G. A., Grove, T. L. & Bryan, W. B. (1993). The influence of water on the petrogenesis of subduction-related igneous rocks. *Nature* **365**, 332–334.

Grove, T. L. & Bryan, W. B. (1983). Fractionation of pyroxene-phyric MORB at low pressure: an experimental study. *Contributions to Mineralogy and Petrology* **84**, 293–309.

Grove, T. L. Gerlach, D. C. & Sando, T. W. (1982). Origin of calc-alkaline series lavas at Medicine Lake volcano by fractionation, assimilation and mixing. *Contributions to Mineralogy and Petrology* **80**, 160–182.

Grove, T. L., Kinzler, R. J. & Bryan, W. B. (1992). Fractionation of mid-ocean ridge basalt (MORB). Mantle flow and melt generation at mid-ocean ridges. In: Phipps Morgan, J., Blackman, D. K. & Sinton, J. M. (eds) *Mantle Flow and Melt Generation at Mid-Ocean Ridges. Geophysical Monograph, American Geophysical Union* **71**, 281–310.

Hekinian, R., Bideau, D., Francheteau, J., Cheminee, J. L., Armijo, R., Lonsdale, P. & Blum, N. (1993). Petrology of the East Pacific Rise crust and upper mantle exposed in Hess Deep, Eastern Equatorial Pacific. *Journal of Geophysical Research* **98**, 8069–8094.

Herzberg, C. T. (1972). Stability fields of plagioclase and spinel-lherzolite. *Progress in Experimental Petrology, Natural Environment Research Council Publications* **D.2**, 145–148.

Herzberg, C. (2004). Geodynamic information in peridotite petrology. *Journal of Petrology* **45**.

Herzberg, C. & O'Hara, M. J. (1998). Phase equilibrium constraints on the origin of basalts, picrites, and komatiites. *Earth-Science Reviews* **44**, 39–79.

Herzberg, C. & O'Hara, M. J. (2002). Plume-associated ultramafic magmas of Phanerozoic age. *Journal of Petrology* **43**, 1857–1883.

Irvine, T. N. (1976). Metastable liquid immiscibility and MgO–FeO–SiO$_2$ fractionation patterns in the system Mg$_2$SiO$_4$–Fe$_2$SiO$_4$–CaAl$_2$Si$_2$O$_8$–KAlSi$_3$O$_8$–SiO$_2$. *Carnegie Institution of Washington Yearbook* **75**, 597–611.

Juster, T. C., Grove, T. L. & Perfit, M. R. (1989). Experimental constraints on the generation of FeTi basalts, andesites, and rhyodacites at the Galapagos Spreading Center, 85°W and 95°W. *Journal of Geophysical Research* **94**, 9251–9274.

Kelemen, P. B., Shimizu, N. & Salters, V. J. M. (1995). Extraction of mid-ocean-ridge basalt from the upwelling mantle by focused flow of melt in dunite channels. *Nature* **375**, 747–753.

Kelemen, P. B., Braun, M. & Hirth, G. (2000). Spatial distribution of melt conduits in the mantle beneath oceanic spreading ridges: observations from the Ingalls and Oman ophiolites. *Geochemistry, Geophysics, Geosystems* **1**, paper number 1999GC000012.

Kempton, P. D., Fitton, J. G., Saunders, A. D., Nowell, G. M., Taylor, R. N., Hardarson, B. S. & Pearson, G. (2000). The Iceland plume in space and time: a Sr–Nd–Pb–Hf study of the North Atlantic rifted margin. *Earth and Planetary Science Letters* **177**, 255–271.

Kennedy, A. K., Grove, T. L. & Johnson, R. W. (1990). Experimental and major element constraints on the evolution of lavas from Lihir Island, Papua New Guinea. *Contributions to Mineralogy and Petrology* **104**, 722–734.

Kinzler, R. J. & Grove, T. L. (1985). Crystallization and differentiation of Archean komatiite lavas from northeast Ontario: phase equilibrium and kinetic studies. *American Mineralogist* **70**, 40–51.

Kinzer, R. J. & Grove, T. L. (1992). Primary magmas of mid-ocean ridge basalts 1. Experiments and methods. *Journal of Geophysical Research* **97**, 6885–6906.

Klein, E. M. & Langmuir, C. H. (1987). Global correlations of ocean ridge basalt chemistry with axial depth and crustal thickness. *Journal of Geophysical Research* **92**, 8089–8115.

Koga, K. T., Kelemen, P. B. & Shimizu, N. (2001). Petrogenesis of the crust–mantle transition zone and the origin of lower crustal wehrlite in the Oman ophiolite. *Geochemistry, Geophysics, Geosystems* **2**, paper number 2000GC000132.

Kornprobst, J. (1969). Le massif ultrabasique des Beni Bouchera (Rif Interne, Maroc): étude des péridotites de haute température et de haute pression, et des pyroxénolites, à grenat ou sans grenat. *Contributions to Mineralogy and Petrology* **23**, 283–322.

Langmuir, C. H. (1989). Geochemical consequences of in situ crystallization. *Nature* **340**, 199–205.

Langmuir, C. H., Bender, J. F. & Batiza, R. (1986). Petrological and tectonic segmentation of the East Pacific Rise, 5°30′–14°30′N. *Nature* **322**, 422–429.

Langmuir, C. H., Klein, E. M. & Plank, T. (1992). Petrology systematics of mid-ocean ridge basalts: constraints on melt generation beneath ocean ridges. In: Phipps Morgan, J., Blackman, D. K. & Sinton, J. M. (eds) *Mantle Flow and Melt Generation at Mid-Ocean Ridges. Geophysical Monograph, American Geophyisical Union* **71**, 183–280.

Lehnert, K. A., Su, Y., Langmuir, C. H., Sarbas, B. & Nohl, U. (2000). A global geochemical database structure for rocks. *Geochemistry, Geophysics, Geosystems* **1**, paper number 1999GC000026.

Libourel, G., Boivin, P. & Biggar, G. M. (1989). The univariant curve liquid = forsterite + anorthite + diopside in the system CMAS at 1

bar: solid solutions and melt structure. *Contributions to Mineralogy and Petrology* **102**, 406–421.

Lippard, S. J., Shelton, A. W. & Gass, I. G. (1986). *The Ophiolite of Northern Oman. Geological Society, London, Memoirs* **11**, 178 pp.

Longhi, J. (1987). Liquidus equilibria and solid solution in the system $CaAl_2Si_2O_8–Mg_2SiO_4–CaSiO_3–SiO_2$ at low pressure. *American Journal of Science* **287**, 265–331.

Macdonald, K. C. (1982). Mid-ocean ridges: fine scale tectonic, volcanic and hydrothermal processes within the plate boundary zone. *Annual Review of Earth and Planetary Sciences* **10**, 155–190.

Macdonald, K. C., Fox, P. J., Perram, L. J., Eisen, M. F., Haymon, R. M., Miller, S. P., Carbotte, S. M., Cormier, M.-H. & Shor, A. N. (1988). A new view of the mid-ocean ridge from the behaviour of ridge-axis discontinuities. *Nature* **335**, 217–225.

Maclennan, J., McKenzie, D., Grönvold, K. & Slater, L. (2001). Crust accretion under northern Iceland. *Earth and Planetary Science Letters* **191**, 295–310.

Maclennan, J., McKenzie, D., Grönvold, K., Shimizu, N., Eiler, J. M. & Kitchen, N. (2003). Melt mixing and crystallization under Theistareykir, NE Iceland. *Geochemistry, Geophysics, Geosystems* **4**, paper number 2003GC000558.

Mahood, G. A. & Baker, D. R. (1986). Experimental constraints on depths of fractionation of mildly alkalic basalts and associated felsic rocks: Pantelleria, Strait of Sicily. *Contributions to Mineralogy and Petrology* **93**, 251–264.

McKenzie, D. & Bickle, M. J. (1988). The volume and composition of melt generated by extension of the lithosphere. *Journal of Petrology* **29**, 625–679.

Melson, W. G., Byerly, G. R., Nelson, J. A., O'Hearn, T., Wright, T. L. & Vallier, T. (1977). A catalogue of the major element geochemistry of abyssal volcanic glasses. *Smithsonian Contributions to Earth Sciences* **19**, 31–60.

Melson, W. G., O'Hearn, T. & Jarosewich, E. (2002). A data brief on the Smithsonian abyssal volcanic glass data file. *Geochemistry, Geophysics, Geosystems* **3**, paper number 2001GC000249.

Michael, P. J. (1995). Regionally distinctive sources of depleted MORB: evidence from trace elements and H_2O. *Earth and Planetary Science Letters* **131**, 301–320.

Michael, P. J. & Chase, R. L. (1987). The influence of primary magma composition, H_2O and pressure on mid-ocean ridge basalt differentiation. *Contributions to Mineralogy and Petrology* **96**, 245–263.

Michael, P. J. & Cornell, W. C. (1998). Influence of spreading rate and magma supply on crystallization and assimilation beneath mid-ocean ridges: evidence from chlorine and major element chemistry of mid-ocean ridge basalts. *Journal of Geophysical Research* **103**, 18325–18356.

Muller, M. R., Minshull, T. A. & White, R. S. (1999). Segmentation and melt supply at the Southwest Indian Ridge. *Geology* **27**, 867–870.

Muller, M. R., Minshull, T. A. & White, R. S. (2000). Crustal structure of the Southwest Indian Ridge at the Atlantis II Fracture Zone. *Journal of Geophyscial Research* **105**, 25809–25828.

Murton, B., Taylor, R. N. & Thirlwall, M. F. (2002). Plume–ridge interaction: a geochemical perspective from the Reykjanes Ridge. *Journal of Petrology* **43**, 1987–2012.

Navin, D. A., Peirce, C. & Sinha, M. C. (1998). The RAMESSES experiment; II, Evidence for accumulated melt beneath a slow spreading ridge from wide-angle refraction and multichannel reflection seismic profiles. *Geophysical Journal International* **135**, 746–772.

Nicolas, A. (1989). *Structures of Ophiolites and Dynamics of Oceanic Lithosphere*. Dordrecht: Kluwer Academic, 367 pp.

Nicolas, A., Reuber, I. & Benn, K. (1988). A new magma chamber model based on structural studies in the Oman ophiolites. *Tectonophysics* **151**, 87–105.

Niu, Y. (1997). Mantle melting and melt extraction processes beneath ocean ridges: evidence from abyssal peridotites. *Journal of Petrology* **38**, 1047–1074.

Niu, Y. & Batiza, R. (1991). An empirical method for calculating melt compositions produced beneath mid-ocean ridges: application for axis and off-axis melting. *Journal of Geophysical Research* **96**, 21753–21777.

Obata, M. (1980). The Ronda peridotite: garnet-, spinel-, and plagioclase-lherzolite facies and the *P–T* trajectories of a high-temperature mantle intrusion. *Journal of Petrology* **23**, 296–298.

O'Donnell, T. H. & Presnall, D. C. (1980). Chemical variations of the glass and mineral phases in basalts dredged from 25°–30°N along the Mid-Atlantic ridge. *American Journal of Science* **280**, 845–868.

O'Hara, M. J. (1968a). Are ocean floor basalts primary magmas? *Nature* **220**, 683–686.

O'Hara, M. J. (1968b). The bearing of phase equilibria studies in synthetic and natural systems on the origin of basic and ultrabasic rocks. *Earth-Science Reviews* **4**, 69–133.

O'Hara, M. J. & Herzberg, C. (2002). Interpretation of trace element and isotope features of basalts: relevance of field relations, petrology, major element data, phase equilibria, and magma chamber modeling in basalt petrogenesis. *Geochimica et Cosmochimica Acta* **66**, 2167–2191.

O'Hara, M. J. & Schairer, J. F. (1963). The join diopside–pyrope at atmospheric pressure. *Carnegie Institution of Washington Yearbook* **62**, 107–115.

Osborn, E. F. & Tait, D. B. (1952). The system diopside–forsterite–anorthite. *American Journal of Science* **250A**, 413–433.

Pallister, J. S. & Hopson, C. A. (1981). Samail ophiolite plutonic suite: field relations, phase relations, cryptic layering and layering, and a model of a spreading ridge magma chamber. *Journal of Geophysical Research* **86**, 2593–2644.

Perfit, M. R., Fornari, D. J., Ridley, W. I., Kirk, P. D., Casey, J., Kastens, K. A., Reynolds, J. R., Edwards, M., Desonie, D., Shuster, R. & Paradis, S. (1996). Recent volcanism in the Siqueiros transform fault: picritic basalts and implications for MORB magma genesis. *Earth and Planetary Science Letters* **141**, 91–108.

Presnall, D. C., Dixon, S. A., Dixon, J. R., O'Donnell, T. H., Brenner, N. L., Schrock, R. L. & Dycus, D. W. (1978). Liquidus phase relations on the join diopside–forsterite–anorthite from 1 atm to 20 kbar: their bearing on the generation and crystallization of basaltic magma. *Contributions to Mineralogy and Petrology* **66**, 203–220.

Presnall, D. C., Dixon, J. R., O'Donnell, T. H. & Dixon, S. A. (1979). Generation of mid-ocean ridge tholeiites. *Journal of Petrology* **20**, 3–35.

Rhodes, J. M., Dungan, M. A., Blanchard, D. P. & Long, P. E. (1979). Magma mixing at mid-ocean ridges: evidence from basalts drilled near 22°N on the Mid-Atlantic Ridge. *Tectonophysics* **55**, 35–61.

Roeder, P. L. (1974). Activity of iron and olivine solubility in basaltic liquids. *Earth and Planetary Science Letters* **23**, 397–410.

Schairer, J. F. (1954). The system $K_2O–MgO–Al_2O_3–SiO_2$. I. Results of quenching experiments on four joins in the tetrahedron cordierite–forsterite–leucite–silica and on the join cordierite–mullite–potash feldspar. *Journal of the American Ceramic Society* **37**, 501–533.

Schairer, J. F. & Yoder, H. S., Jr (1967). The system albite–anorthite–forsterite at 1 atmosphere. *Carnegie Institution of Washington Yearbook* **65**, 204–209.

Scheirer, D. S., Forsyth, D. W., Cormier, M.-H. & Macdonald, K. C. (1998). Shipboard geophysical indications of asymmetry and melt

production beneath the East Pacific Rise near the MELT experiment. *Science* **280**, 1221–1224.

Shen, Y. & Forsyth, D. W. (1992). The effects of temperature- and pressure-dependent viscosity on three-dimensional passive flow of the mantle beneath a ridge–transform system. *Journal of Geophysical Research* **97**, 19717–19728.

Shen, Y. & Forsyth, D. W. (1995). Geochemical constraints on initial and final depths of melting beneath mid-ocean ridges. *Journal of Geophyscial Research* **100**, 2211–2237.

Sisson, T. W. & Grove, T. L. (1993). Experimental investigations of the role of H_2O in calc-alkaline differentiation and subduction zone magmatism. *Contributions to Mineralogy and Petrology* **113**, 143–166.

Slater, L., McKenzie, D., Grönvold, K. & Shimizu, N. (2001). Melt generation and movement beneath Theistareykir, NE Iceland. *Journal of Petrology* **42**, 321–354.

Sleep, N. (1975). Formation of the oceanic crust: some thermal constraints. *Journal of Geophysical Research* **80**, 4037–4042.

Sun, S.-s., Tatsumoto, M. & Schilling, J.-G. (1975). Mantle plume mixing along the Reykjanes Ridge axis: lead isotopic evidence. *Science* **190**, 143–147.

Taylor, R. N., Thirlwall, M. F., Murton, B. J., Hilton, D. R. & Gee, M. A. M. (1997). Isotopic constraints on the influence of the Icelandic plume. *Earth and Planetary Science Letters* **148**, E1–E8.

Thompson, G., Bryan, W. B. & Melson, W. G. (1980). Geological and geophysical investigations of the mid-Cayman rise spreading center: geochemical variation and petrogenesis of basalt glasses. *Journal of Geology* **88**, 41–55.

Thy, P. & Lofgren, G. E. (1992). Experimental constraints on the low-pressure evolution of transitional and mildly alkalic basalts: multisaturated liquids and coexisting augites. *Contributions to Mineralogy and Petrology* **112**, 196–202.

Thy, P. & Lofgren, G. E. (1994). Experimental constraints on the low-pressure evolution of transitional and mildly alkalic basalts: the effect of Fe–Ti oxide minerals and the origin of basaltic andesites. *Contributions to Mineralogy and Petrology* **116**, 340–351.

Tormey, D. R., Grove, T. L. & Bryan, W. B. (1987). Experimental petrology of normal MORB near the Kane Fracture Zone: 22°–25°N, Mid-Atlantic Ridge. *Contributions to Mineralogy and Petrology* **96**, 121–139.

Ussler, W., III & Glazner, A. F. (1989). Phase equilibria along a basalt–rhyolite mixing line: implications for the origin of calc-alkaline intermediate magmas. *Contributions to Mineralogy and Petrology* **101**, 232–244.

Walker, D., Shibata, T. & DeLong, S. E. (1979). Abyssal tholeiites from the Oceanographer Fracture Zone. II. Phase equilibria and mixing. *Contributions to Mineralogy and Petrology* **70**, 111–125.

Walter, M. J. & Presnall, D. C. (1994). Melting behavior of simplified lherzolite in the system $CaO–MgO–Al_2O_3–SiO_2–Na_2O$ from 7 to 35 kbar. *Journal of Petrology* **35**, 329–359.

Weaver, J. & Langmuir, C. (1990). Calculation of phase equilibrium in mineral–melt systems. *Computers and Geosciences* **16**, 1–19.

White, R. S., Detrick, R. S., Sinha, M. C. & Cormier, M. H. (1984). Anomalous seismic crustal structure of oceanic fracture zones. *Geophysical Journal of the Royal Astronomical Society* **79**, 779–798.

White, R. S., Minshull, T. A., Bickle, M. J. & Robinson, C. J. (2001). Melt generation at very slow-spreading oceanic ridges: constraints from geochemical and geophysical data. *Journal of Petrology* **42**, 1171–1196.

Yang, H.-J., Kinzler, R. J. & Grove, T. L. (1996). Experiments and models of anhydrous, basaltic olivine–plagioclase–augite saturated melts from 0·001 to 10 kbar. *Contributions to Mineralogy and Petrology* **124**, 1–18.

Yoder, H. S., Jr (1965). Diopside–anorthite–water at five and ten kilobars and its bearing on explosive volcanism. *Carnegie Institution of Washington Yearbook* **64**, 82–89.